INPE ePrint: sid.inpe.br/yolanda/2004/12.08.14.16 v1 2004-12-09

Electrochemical Insertion of lithium into doped diamond grown on carbon felt substrates

E. C. Almeida[1], J. M. Rosolen[2], V. J. Trava-Airoldi[1], N. G. Ferreira[3]

[1]INPE, C.P. 515 -12245-970, São José dos Campos, Brazil[2]DQ, FFCLRP, Universidade de São Paulo, 14040-901 Ribeirão Preto, Brazil[3]Divisão de Materiais, AMR /CTA, 12228-904, São José dos Campos, Brazil
erica@las.inpe.br

Abstract

This paper summarizes the preliminary results of lithium electrochemical intercalation results into boron-doped diamond films grown on no woven of carbon fiber or carbon felt (BDD/CF electrode). BDD films were grown by Hot Filaments Chemical Vapor Deposition (HFCVD) and characterized from Scanning Electron Microscopy (SEM) and Raman Scattering spectroscopy. The BDD/CF electrodes that contain diamond layer more conductivity, with smaller grains size and in turn more rich of boundary or sp^2 sites present an reversible specific capacity that is much large than the substrate alone, indicating effectively the participation of diamond in the lithium storage. The diamond layer with doping level 10^{19} and 10^{21} provided 160 and 370 $mAh.g^{-1}$ of specific capacity associated with lithium storage, respectively. In the lithium area the results shows that this new class of electrodes can be very useful since the electrodes are free of binder polymer traditionally used in the preparation of lithium battery.

Keywords: Batteries, lithium intercalation, carbon fibers and CVD -diamond

Introduction

Numerous studies on the electrochemical insertion of lithium into various carbon materials have been reported [1-7]. Studies on lithium intercalation into graphite, in particular, have been well established [8-14]. It is known that a maximum of one lithium atom per six carbon atoms can be intercalated when lithium is fully intercalated into graphite. In LiC_6, the intercalated lithium exists as a screened ion between two adjacent graphite layers with the theoretical specific capacity of LiC_6 being 372 mA.h/g.

Recently, carbons with capacities higher than the theoretical value of graphite have been prepared by pyrolyzing organic precursors at heat treatment temperatures below 1000 ºC [15,16]. Some suggestions have been proposed for the extra capacity over the theoretical value of 372 mAh/g, such as lithium occupation of nearest neighbor sites [17], lithium insertion into nanoscopic cavities [18], binding of lithium in the vicinity of the hydrogen atoms [19], additional insertion of lithium at the edge area of graphene layers [20] and at the graphene surface as well [21]. Additional works have been focused on the efect of chemical substituents in carbons, including phosphorus [22], boron [23], and nitrogen [24].

Boron-doping into graphite is one of the well-known methods to improve the discharge capacity of the graphite electrode. The boron atoms at sustitutional sites should not cause a notable distortion of the crystal structure because its atomic size is comparable to that of carbon. Because boron has less electrons than carbon, it acts as an electron acceptor which creates the hole-carrier in the valence band by enhancing the electrical conductivity of graphite and increases its discharge capacity [25].

Recently, we have shown the first study of lithium intercalation for diamond films grown on Mo and on cloth of carbon fibers substrates [26]. This work represents additional contribution for this subject by investigating lithium intercalation into composite diamond electrodes by electrochemical characterization. Boron doped diamond films were grown on no woven of carbon fibers or carbon felt (BDD/CF electrode) with different levels of boron doping. It was studied the lithium intercalation as a function of the boron content. Scanning electron microscopy and Raman spectroscopy were also used to characterize the film morphology and quality.

Experimental

CF samples were produced from polyacrylonitrile (PAN) precursor at different HTT by using temperature steps of 330 K/h under inert atmosphere with nitrogen flow of 1 $L.h^{-1}$, reaching the maximum temperature of 1000 °C, standing at this maximum during 30 min until its cooling down to room temperature.

BDD films were grown by HFCVD technique at 1050 K from 0.5% H_2/CH_4 mixture at a total pressure of 6.5 x 10^3 Pa during 20 hours. The substrates were ultrasonically pre-treated in a mixture of 0.25 μm diamond powder dissolved in hexane for 1 hours. Boron source was obtained from H_2 forced to pass through a bubbler containing B_2O_3 dissolved in methanol. This system permits the control of boron concentration using a flow controller for the gas inlet. For all experiments the desired B/C ratios was controled monitoring the H_2 and $B_2O_3/CH_3OH/H_2$ flows. The doping level studied corresponds to acceptor concentrations in the range of 6.5 x 10^{18} up to 1.5 x 10^{21} cm^{-3}, obtained from Mott-Schottky plots measurements in previous work [27].

The composite electrodes obtained were disks with 8 mm diameter. The electrodes were heated at 120°C for 12 h at 9.10^3 Pa before the assembly on electrochemical cells in the dry-box. The electrochemical characterizations were performed in a coin cell kind of Sagellock, where lithium was used both as the auxiliary and reference electrodes. Two layers of separator (Celgard) were used in the electrochemical cells. The electrolyte used was 1$mol.L^{-1}$ of $LiPF_6$ in a mixture of ethylene carbonate (EC), dimethyl carbonate (DMC) and diethyl carbonate (DEC) (1:1:1 wt, Selectur). Cyclic voltammetry was carry out at a scan rate of 100$\mu V.s^{-1}$ sing a potentiostat/galvanostat EGG/PAR 364. The charge/discharge curves were colleted in galvanostatic mode using a Macpile cycler at a current of 20μA. The discharges of electrodes were carried out until one cut-off of 0.010V versus Li. Top view and cross-section images of BDD/CF films were obtained by SEM from a Jeol equipment JSM-5310. Micro-Raman spectra were recorded by a Renishaw microscope system 2000 in backscattering configuration at room temperature employing 514.5 nm argon-ion laser.

Results and discussion

The surface analysis made by SEM for BDD films have evidence that the variation on surface morphology is associated with the decrease of the growth rate due to boron incorporation. Figures 1A and 1B show the micrograph of CF and BDD/CF electrode with boron doping of 10^{18} part.cm^{-3}, respectively. The Fig.1A shows that surface of CF contains in longitudinal direction a roughness. The cross section of the fiber seens to have a non regular texture with one central concavity. The CF obtained presents diameter of around 10 μm, resistively determined by four-probe method is 0.96 Ω.cm, d_{002} = 4.34 Å and L_{002} = 11.6 Å determined by the XRD [28]. SEM images demonstrated also that individual fibers in surface of the felt were completely covered (surface and cap) by the diamond crystals (Fig. 1B). The grains are faceted with symmetrical and smooth faces with uniform texture and a surface morphology with predominant (111) orientation, but the grain sizes are not identical. For all sets of sample studied we have systematically observed that the average grain size decreases with the increase of boron content for the same substrate.

The quality and doping level of the diamond films grown in CF were studied by Raman spectroscopy. A drastic change of Raman spectra of diamond films with different doping levels was observed. Figures 2 a,b,c show the Raman spectra with an acceptor concentrations of around 10^{18} ,10^{19} and 10^{21} cm^{-3}, respectively. The results reveal that the peak intensity at 1332 cm^{-1} corresponding to the transversal mode (related to the sp^3 bonds) of the diamond decreases as the boron concentration increases. Nevertheless, a wide band arises approximately 1220 cm^{-1} and increases as the boron concentration increase, as shown in Figure 2c. The decrease of the zone center phonon peak at 1332 cm^{-1} and the appearance of the broad peak at 1220 cm^{-1} was attributed to the relaxation of the $\Delta\kappa=0$ selection rule caused by the small coherence length of diamond crystallites [29-31]. A small coherence length is expected because of wideness of the distribution of grains size decreases with reduction of grains size, as in fact, we have observed in the SEM pictures of samples.

Figures 3 shows the discharge (negative polarization) and charge (positive polarization) curves of the CF and BDD/CF electrodes with an acceptor concentration of around 10^{18} to 10^{21} part.cm^{-3}. The table 1 shows the values of Faradic charge during cathodic (discharge) and anodic (charge) polarization and the fraction of charge of electrode that can not be used in the lithium storage (irreversible capacity), i. e., the diference between the specific capacity obtained during lithium extraction (increase of voltage) and cathodic polarization (decrease of voltage) divide by the charge specific capacity (increase of voltage).

All electrodes present, as expected, an voltage variation observed in figure 3 is predominantly resulting of the ohmic-drop, charging/discharging of double-layer and the variation of chemical potential of the electrons (Fermi level) and intercalated ions as well formation of solid layer insulator permeable to ions that cover the surface of carbon resulting from decomposition of electrolyte-SEI [32,33]. Deposition of lithium metalic in the carbon electrode are expected only in potential beyond the 0V vs Li. The two first contributions occurs in the first seconds of polarization. Afterward, the voltage profile is governed by the variation of Fermi level and the chemical potential of electrons such that the electronic and structural propriety of composite determine the behavior of voltage profile with amount of lithium storied in the bulk of material. The formation of SEI

occurs in carbon materials often at about 1.0 and 0.5 V vs Li and its responsible for lost charge in the cycle if we considered that all lithium insered can be extracted in the opposite polarization.

The CF electrode (Fig. 3a) shows a voltage profile well symmetric without presence of plateau. The voltage profile of the CF seems with those determined for pitch-based carbon fiber (d_{002} in the range of 3.4Å that present specific capacity and irreversible capacity similar to the table I) [34]. The lithium storage in the CF studied here may be occuring, thus, in the edges of fibers and in the interlayer space along the c-axis. The irreversible charge (table 1) is associated to formation of SEI.

For the case of the BDD/CF electrodes the voltage profile is quite different of substrate, indicating that diamond act effectively in the process of lithium storage in the composite electrode. The voltage profile and specific capacities changes as Boron concentration or conductivity diamond or average grain size that compound the diamond layer.

Most recently, we have demonstrated that is possible the intercalation of lithium in diamonds deposited on Mo substrated by electro-polarization in Li-ions battery electrolyte [26]. We believe that lithium is insered in the structure and in the boundary between grains that are rich of sp^2 sites. For insertion of lithium in a compound is important the formation of concentration gradient in the interface and an electron mobility such that the electroneutrality of Li insered ions, an essencial condition to ionic diffusing inside the structure. If the material is an insulator the Li eletrointercalation can occurs since the electrons arrived in the interface. Typical example, is the olivine, an electrolyte that can be used also as electrode in Li-ion battery if its surface is cover by carbon [35]. In this context, as smaller are the grains, in turn, better will be the intercalation of lithium. All these statements are supported in Fig. 3.

The curves of figure 3 reveals that differences observed in the curves as well as the specific capacity are correlated to storage of lithium in the diamond layer. For the composite electrode prepared with diamond more insulator we observe a discharge capacity that reaches 370 $mAh.g^{-1}$ and a very high irreversible capacity (see fraction of lost charge table 1). The charge capacity that can be associated to effective fraction of lithium that was storage in the electrode is only 90 $mAh.g^{-1}$. This behavior is agreement with the fact that the diamond layer applied in the CF (Fig.3b) is an layer more insulator that other layer and their grains are also larger than the grains found in the other layer (Fig. 3c, d). Thus, the Fig.3b shows that the diamond layer with 10^{18} doping level has a grains size and conductivity that does not a efficient intercalation to the current applied in the electrode. During negative polarization the Faradic charge provide to electrode for the galvanostate was used to decomposition of electrolyte. Other aspect interesting, that can be observed in Fig. 3b is that in 2.0V occurs an increase of voltage. This invertion can be explain as an exfoliation of diamond layer associated to stress provoked insertion of the lithium in the bulk of diamond or the sp^2 sites (boundary of grains). The exfoliation can break the electrode expound new sites for lithium insertion. Exfoliation in graphite has been observed when this material is polarized in electrolytes contain molecules that can be insered inside the planes of crystallite or co-intercalated with Li in the inter-layer planes [36,37].

On the other hand, the composite electrodes that contain diamond layer more conductivity, with smaller grains size and in turn more rich of boundary or sp^2 sites (Fig.3c and 3d) present an reversible specific capacity that is much large than the

substrate alone, indicating effectively the participation of diamond in the lithium storage. The diamond layer with doping level 10^{19} and 10^{21} provided 160 and 370 $mAh.g^{-1}$ of specific capacity associated with lithium storage, respectively. The bulk of diamond and the sp^2 sites that exist in the boundary of diamond grains allows one increase of lithium storage of CF substrate of the 10 $mAh.g^{-1}$ (doping level 10^{19}) and 155 $mAh.g^{-1}$ (doping level 10^{21}). If we take in account the we could represent the lithium insered in the Boron diamond layer (sp^2 sites in the boundary grains more sp^3 sites, sites inside the diamond structure) as $Li_x(B_zC_{1-z})_6$, for the diamond layer studied x is about 0.48 and 0.03 moles of lithium, respectively for Boron doping level 10^{21} and 10^{19}.

The evidence of the increase of sp^2 sites respect to sp^3 sites in the B-diamond layer with smaller grains 10^{21} appears also in the voltage profile. The voltage profile of Fig. 3d remember that found for graphite [38,39]. This detail may suggest that the lithium is has been storied in the Boron diamond layer mainly in the sp^2 sites since the diamond layer doped with 10^{21} $part.cm^{-3}$, should have grains favorable to insertion of lithium inside the diamond lattice (sp^3 sites).

Finally, Fig. 4 show the voltamograms of CF electrode and the composite electrode with best capacity to storage lithium detected in Fig. 3. The voltamograms present two intense peaks cathodic and anodic associated effectively by the insertion and extraction of lithium. A higher cathodic peak current is observed for BDD/CF (-0.7 V x Li), compared to the CF substrate (-0.2 V x Li). This behavior indicates the kinetics of lithium insertion /removal in BDD/CF electrode to be the fastest.

Therefore, the results demonstrated that diamond layer grows in carbon substrate has effective participation in the process of lithium storage. The grains size and conductivity of Boron-diamond layer has big influence in this process. Smaller grains and higher electronic conductivity are favorable to increase of capacity of electrode to storage lithium. However, smaller grains increase the electrochemical area that imply in the charge lost with decomposition of electrolyte that results in the SEI.

Conclusions

We have show that BDD/CF is able to lithium storage. In this work the Boron-BDD was used as layer in CF that in the composite electrode seems act as substrate very useful to preparation of electrodes to several electrochemical applications. This BDD layer was understand as layer where are distributive sp^2 sites (boundary grains) and sp^3 sites of diamond. The results suggest that most of lithium is been probably storage in the sp^2 sites of layer, however, an better evidence of this supposition may be found in B-nanodiamond layers grown on CF substrates.

In the lithium area the results shows that this new class of electrodes can be very useful since the electrodes are free of binder polymer traditionally used in the preparation of lithium battery. The results show that boron diamond composite electrode can be become competitive if was find a B-diamond layer that provide an elevated number of sp^2 and sp^3 with good kinetic the intercalation, but with irreversible capacity very smaller that found in table 1. A best understanding of lithium intercalation in BDD layer on Ti as well as the study of composite electrodes on several kind of CF substrates will be carry out.

ACKNOWLEDGEMENTS

We are very grateful M. C. Rezende AMR/CTA by providing the no woven of carbon fibers substrates. We are also grateful to J. Panasiewicz Junior by SEM analysis.

References

[1] K. Tatsumi, N. Iwashita, H. Sakaede, H. Shioyama, S. Higuchi, A. Mabuchi, and H. Fujimoto, J. Electrochem. Soc., 142 (1995) 716 .

[2] Y-G. Wang, Y-C. Chang, S. Ishida, Y. Korai, I. Mochida, Carbon 37 (1999) 969.

[3] K. Guerin, A. Fevrier-Bouvier, S. Flandrois, B. Simon, P. Biensan, Electrochim. Acta 45 (2000) 1607.

[4] E. Buiel, J.R. Dahn. , Electrochim. Acta 45 (1999) 121.

[5] G. B. Appetecchi, F. Croce, R. Marassi, L. Persi, P. Romagnoli, B. Scrosati , Electrochim. Acta 45 (1999) 23.

[6] K. Sato, M. Noguchi, A. Demachi, N. Oki, M. Endo, Science 264 (1994) 556.

[7] A. K. Holliday, G. Hughes, S.M Walker, Comprehensive inorganic chemistry. In: Trotman-Dickenson AF, editor, Carbon, Oxford: Pergamon Press, 1973, pp. 1173–294.

[8] H. Wang, T. Ikeda, K. Fukuda, M. Yoshio , J Power Source 83 (1999) 141.

[9] Z. Liu, A.Yu, J.Y. Lee,. J Power Source 81–82 (1999) 187.

[10] R. McMillan, H. Slegr, Z. X. Su, W. Wang, J Power Source 81–82 (1999) 20.

[11] A. M. Andersson, K. Edstrom, J. O. Thomas. , J Power Source 81–82 (1999) 8.

[12] R. Yazami. , Electrochim. Acta 45 (1999) 87.

[13] W . Xing, J. R. Dahn , J. Electrochem. Soc 144 (1997) 1195.

[14] T. Ohzuku, Y. Iwakoshi, K. Sawai, J. Electrochem. Soc. 140 (1993) 2490.

[15] H.-Q Xiang, S.-B. Fang, Y.-Y. Jiang, Solid State Ionics 148 (2002) 35.

[16] R. Yazami, M. Deschamps, J. Power Sources 54 (1995) 153.

[17] K. Sato, M. Noguchi, A. Demachi, N. Oki, M. Endo, Science 264 (1994) 556.

[18] K. Tokumitsu, A. Mabuchi, H. Fujimoto, T. Kasuh, J. Electrochem. Soc. 143 (1996) 2235.

[19] J. R. Dahn, T. Zheng, Y. Liu, J. S. Xue, Science 270 (1995) 590.

[20] H-Q. Xiang, S-B. Fang, Y-Y. Jiang, J. Electrochem. Soc. 144 (1997) L187.

[21] Y. Matsumura, S. Wang, J. Mondori, Carbon 33 (1995) 1457.

[22] T. Mayer, R. W. Pekala, R. L. Morrison, L. Kaschmitter, US Pat. No. 5358802, 1994.

[23]M. Morita, T. Hanada, H. Tsusumi, Y. Matsuda, M. kawaguchi, J. Electrochem. Soc. 139 (1992) 1227.

[24] M. Ishikawa, T. Nakamura, M. Morita, Y. Matsuda, S. Tsujioka, T. Kawashima, J. Power Sources 55 (1995) 127.

[25] A. Marchand, Chem. Phys. Carbon 7 (1971) 155.

[26] N.G. Ferreira , L.L. Mendonca , V.J.T. Airoldi , J.M. Rosolen , Diamond Relat. Mater. 12 (2003)596.

[27] N.G. Ferreira, L.L.G. Silva, E.J. Corat, V.J. Trava-Airoldi, Diamond Relat. Mater . 11 (2002) 1523.

[28] E.C. Almeida, J.M. Rosolen, V.J. Trava-Airoldi, N.G. Ferreira, submitted for publication in Diamond Relat. Mater.

[29] R. J. Zhang, S. T. Lee, Y. M. Lam, Diamond Relat. Mater. 5 (1996) 1288.

[30] R. J. Nemanich, J. T. Glass, G. Lukovsky, R. E. Shroder, J. Va. Sci. Technol. A6, (1988) 1783.

[31] C. L. Clement, F. Zenia, N. A. Ndao, A. Deneuville, New Diamond Front Carbon Technol. 19 (1999) 189.

[32] D. Rahner, S. Machill, K. Siury, J. Power Sources 68 (1997) 69.

[33] Z. Takehara, J. Power Sources 68 (1997) 82.

[34] K. Suzuki, T. Iijima, M. Wakihara, Electrochimica Acta 44 (1999) 2185.

[35] H. Huang, S.C. Yin, L.F. Nazar, Electrochem. Solid-State Lett. 4 (2001) A170.

[36] A.N. Dey, B.P. Sullivan, J. Electrochem. Soc. 117 (1970) 222.

[37] R. Fong, U.V. Sacken, J.R. Dahn, J. Electrochem. Soc. 137 (1990) 2009.

[38] R. Yazami, YF. Reynier, Electrochimica Acta 47 (2002) 1217.

[39] J.R. Dahn, J. Zheng, Y. Liu, J.S. Xue, Science 270 (1995) 590.

Figures Captions

Table I. Results of the first discharge for the BDD/CF electrode with an acceptor concentrations of around 10^{18} to 10^{21} part.cm^{-3}.

Figure 1. Scanning electron micrographs of CF (A) and BDD/CF electrode (B) for a doping level of 10^{18} part.cm^{-3}.

Figure 2. Raman spectra of diamond films grown CF with doping levels of: (a) 10^{18} part.cm^{-3}; (b) 10^{19} part.cm^{-3}; (c) 10^{21} part.cm^{-3}

Figure 3. First charge/discharge at 0.020mA for BDD/CF electrodes.(a) Substrate ; (b,c,d) doping levels from 10^{18} up to 10^{21} part.cm^{-3}.

Figure 4. Cyclic voltammetry with a scan-rate of 0.1 mV.s^{-1}: (a) CF electrode; (b)BDD/CF electrode with 10^{21} part.cm^{-3}

Table I

Sample	Capacity Discharge (mA.h/g)	Irreversible Capacity (mA.h/g)	Irreversible Capacity (%)
BDD/CF ~10^{21} B/C	690	370	46%
BDD/CF ~10^{19} B/C	380	160	58%
BDD/CF ~10^{18} B/C	370	90	76%
CF	150	115	23 %

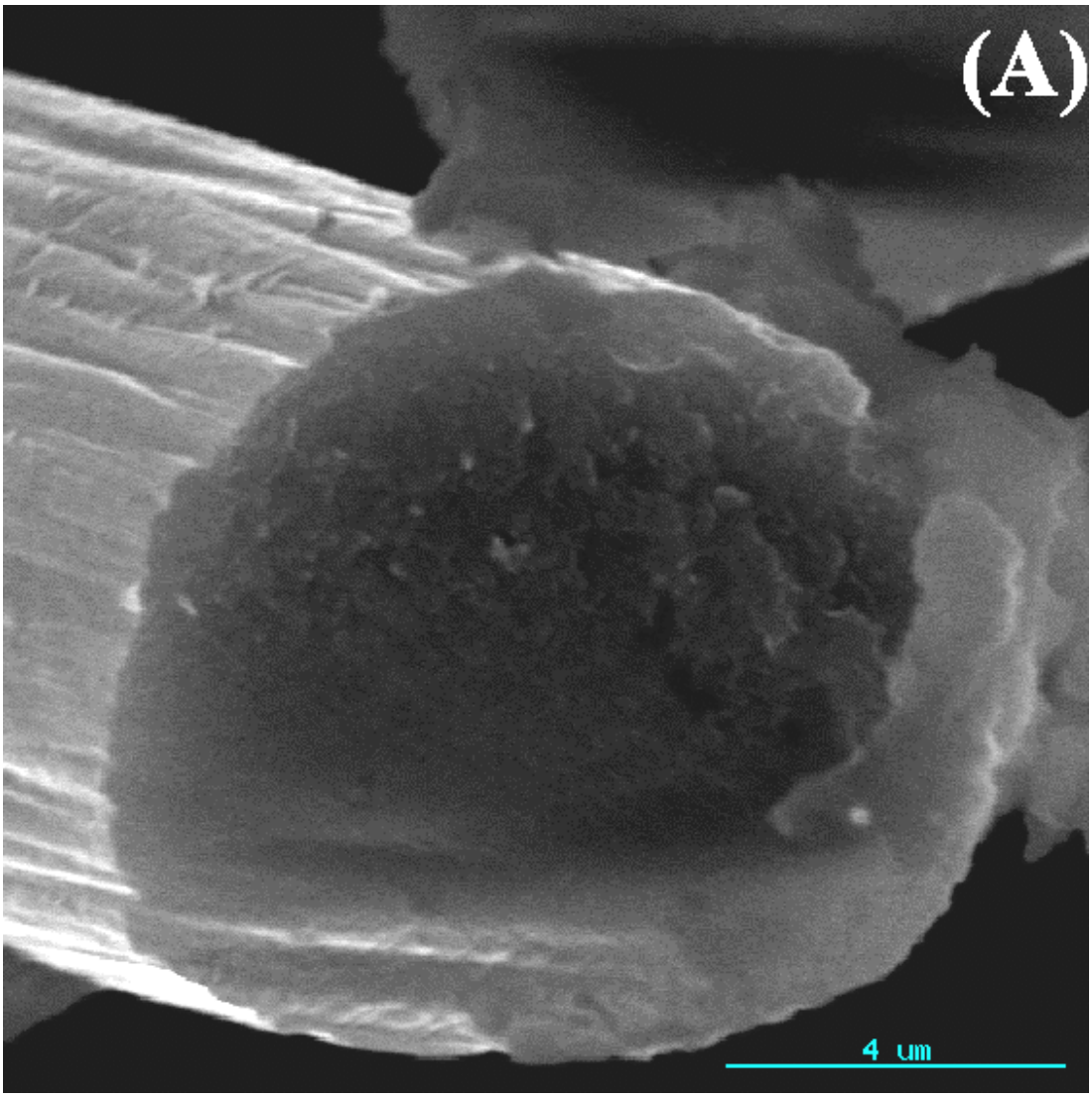

Figure 1 A

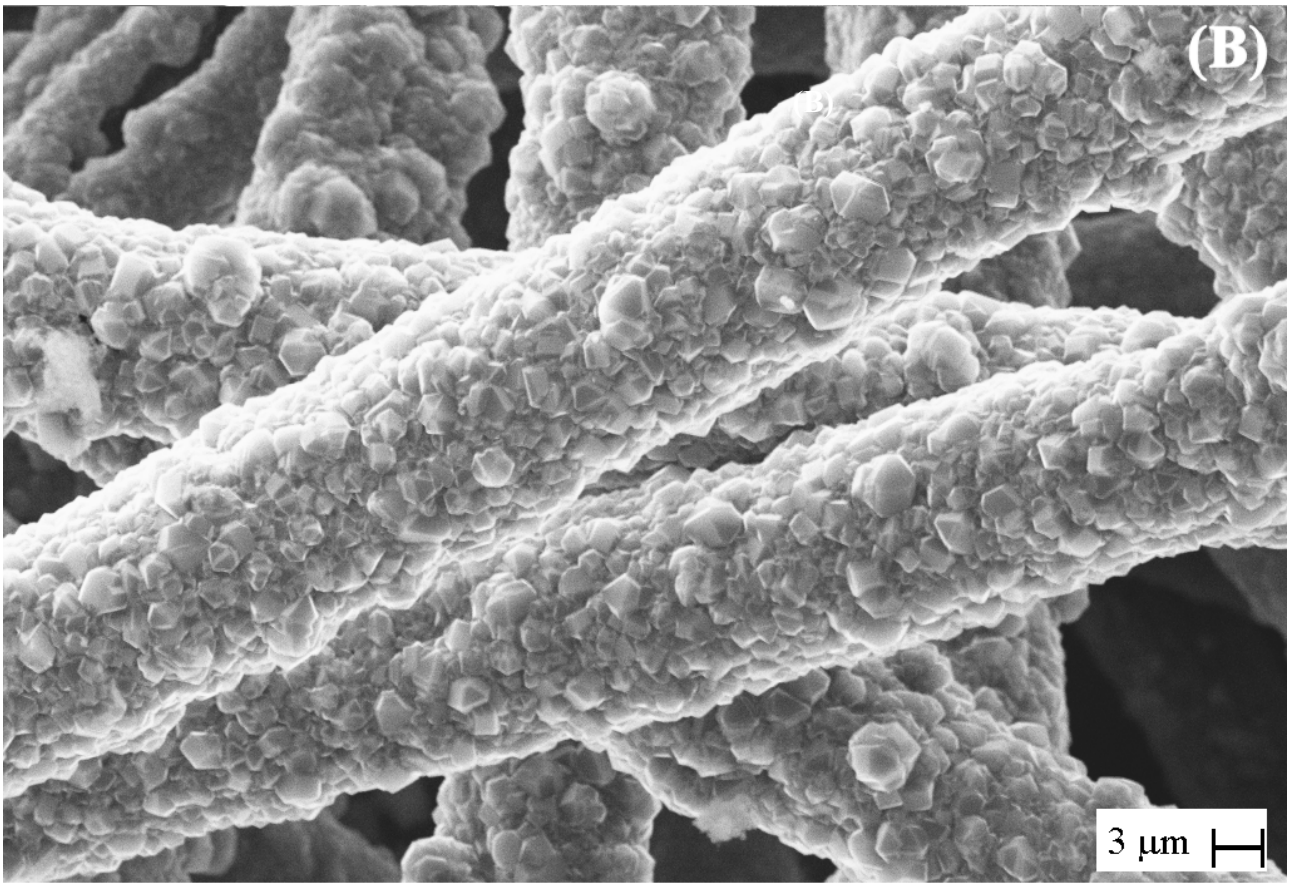

Figure 1 B

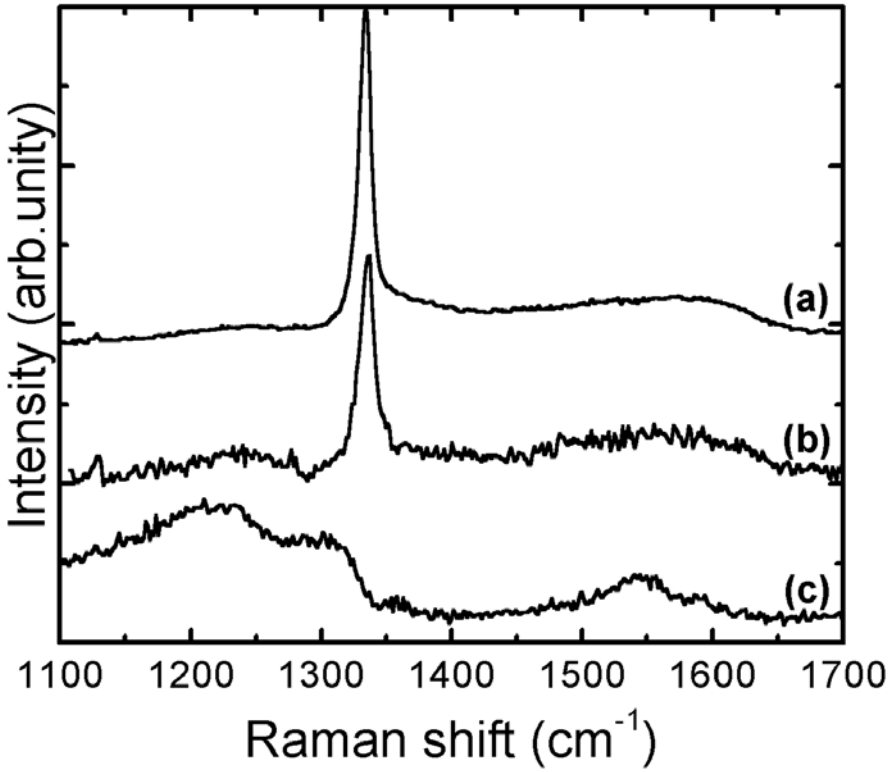
Intensity (arb.unity)
(a)
(b)
(c)
1100
1200
1300
1400
1500
1600
1700
Raman shift (cm-1)

Figure 2

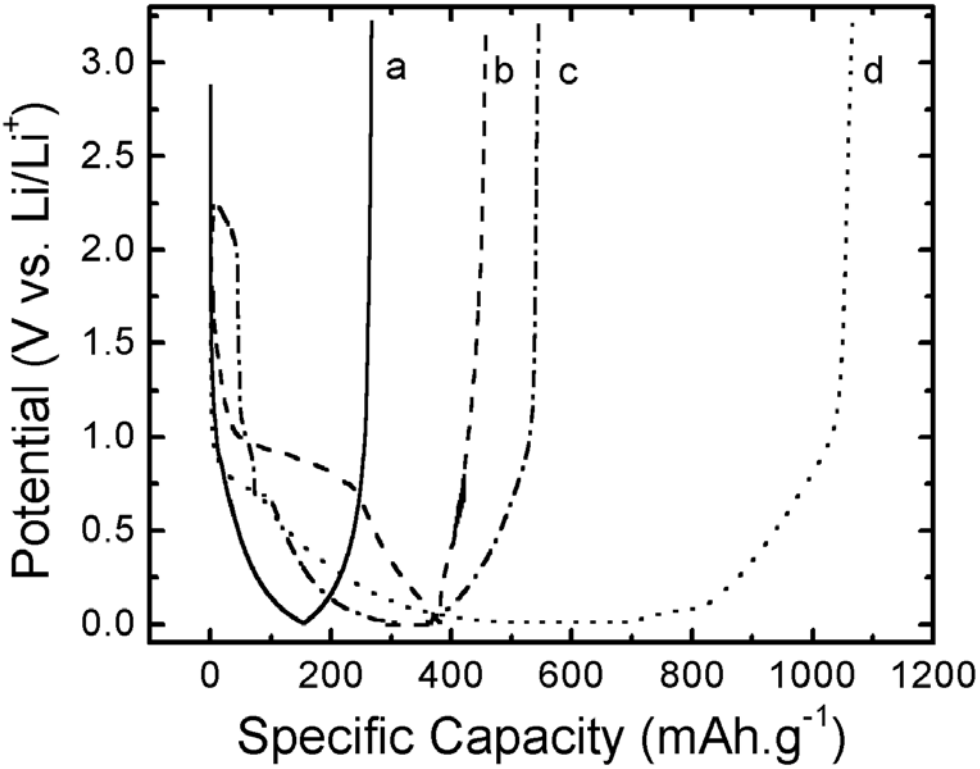
Potential (V vs. Li/Li+)
Specific Capacity (mAh.g-1)
a
b
c
d
0.0
0.5
1.0
1.5
2.0
2.5
3.0
0
200
400
600
800
1000
1200

Figure 3

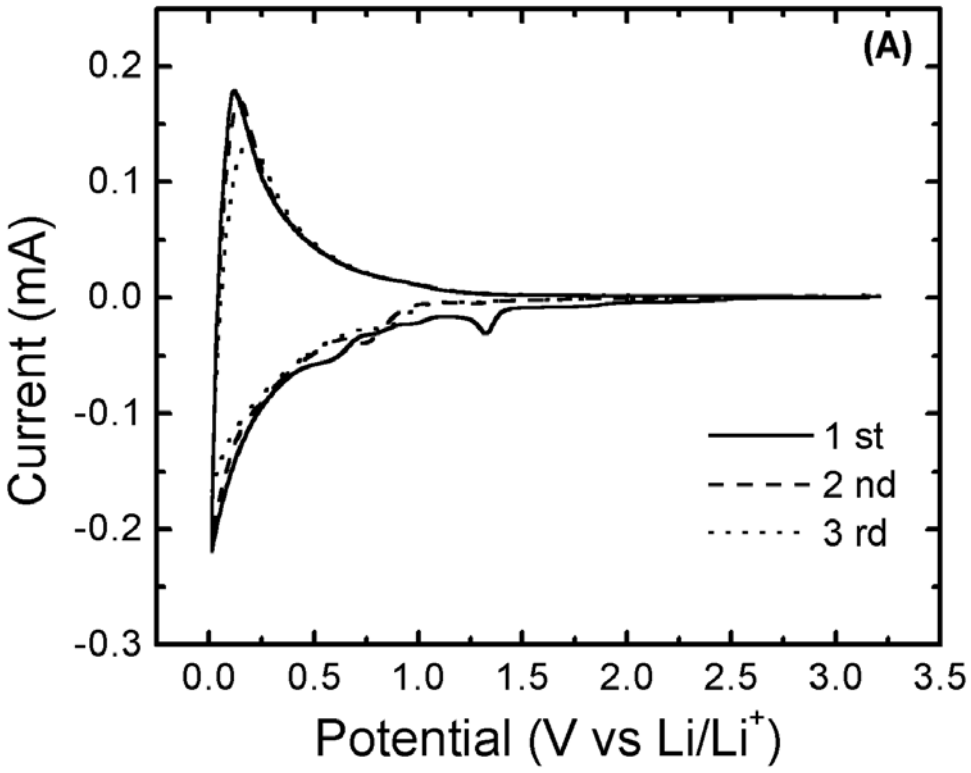
(A)
Current (mA)
Potential (V vs Li/Li+)
1 st
2 nd
3 rd
0.2
0.1
0.0
-0.1
-0.2
-0.3
0.0
0.5
1.0
1.5
2.0
2.5
3.0
3.5

Figure 4 a

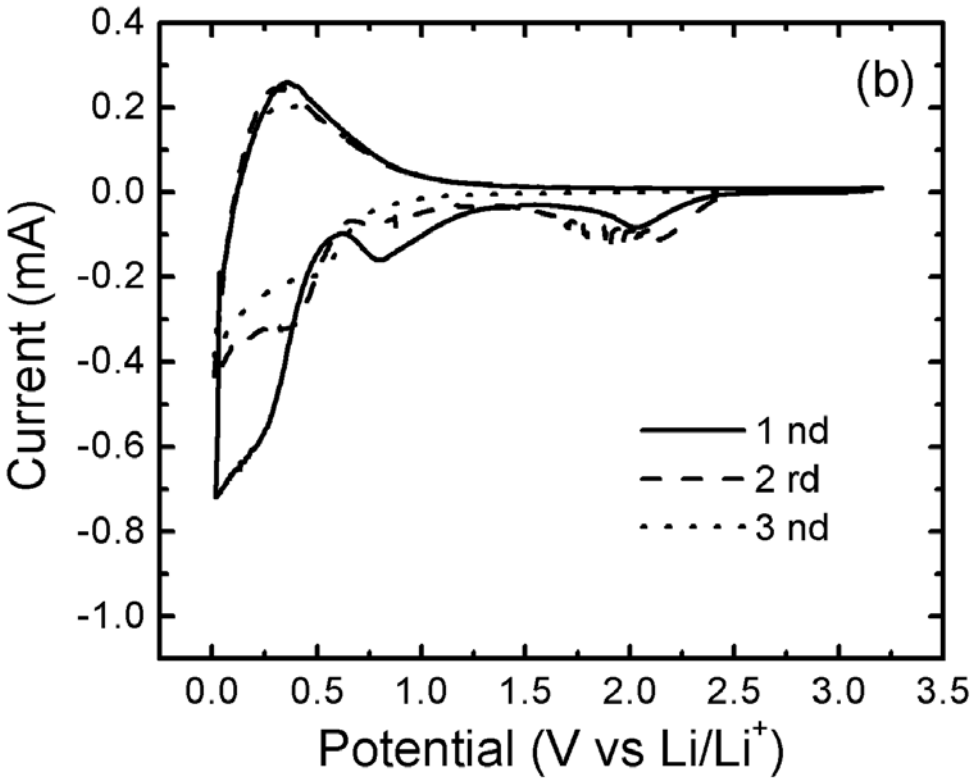
(b)
Current (mA)
Potential (V vs Li/Li+)
1 nd
2 rd
3 nd
0.4
0.2
0.0
-0.2
-0.4
-0.6
-0.8
-1.0
0.0
0.5
1.0
1.5
2.0
2.5
3.0
3.5

Figure 4 b